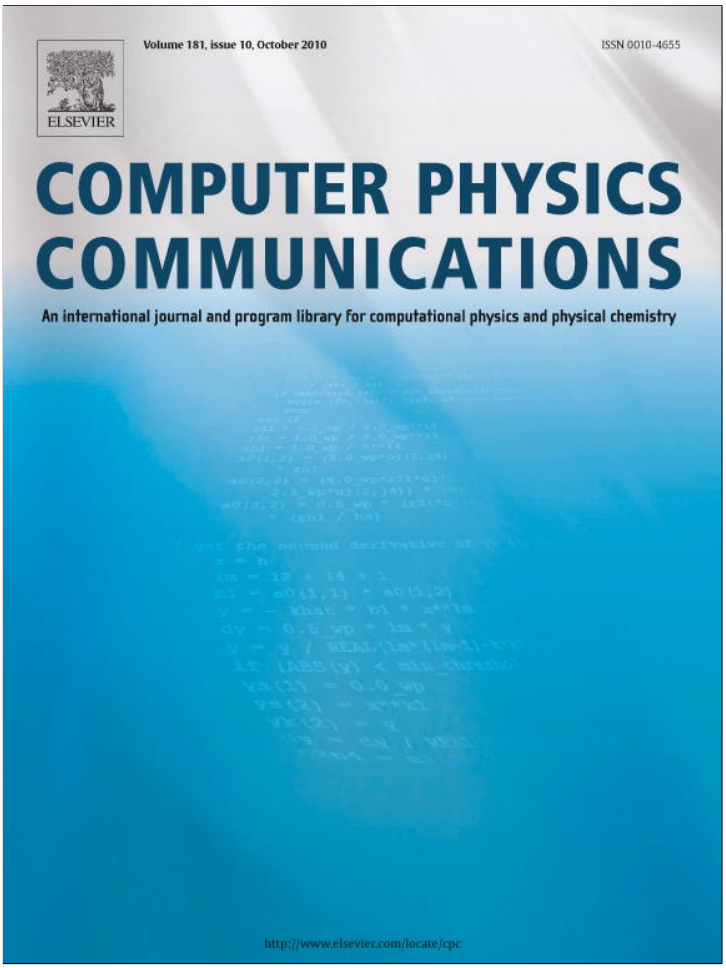

Computer Physics Communications 181 (2010) 1727–1737

Contents lists available at ScienceDirect

Computer Physics Communications

www.elsevier.com/locate/cpc

Two-stage continuation algorithms for Bloch waves of Bose–Einstein condensates in optical lattices

C.-S. Chien [a,1], S.-L. Chang [b,*], Biao Wu [c]

[a] Department of Computer Science and Information Engineering, Ching-Yun University, Jungli 320, Taiwan
[b] Department of Computer Science and Information Engineering, Southern Taiwan University, Tainan 710, Taiwan
[c] International Center for Quantum Materials, Peking University, Beijing 100871, China

ARTICLE INFO

Article history:
Received 4 February 2010
Received in revised form 3 June 2010
Accepted 18 June 2010
Available online 30 June 2010

Keywords:
Bloch bands
Bloch surfaces
Numerical continuation
Bifurcation

ABSTRACT

Bloch waves of Bose–Einstein condensates (BEC) in optical lattices are extremum nonlinear eigenstates which satisfy the time-independent Gross–Pitaevskii equation (GPE). We describe an efficient Taylor predictor–Newton corrector continuation algorithm for tracing solution curves of parameter-dependent problems. Based on this algorithm, a novel two-stage continuation algorithm is developed for computing Bloch waves of 1D and 2D Bose–Einstein condensates (BEC) in optical lattices. We split the complex wave function into the sum of its real and imaginary parts. The original GPE becomes a couple of two nonlinear eigenvalue problems defined in the real domain with periodic boundary conditions. At the first stage we use the chemical potential μ as the continuation parameter. The Bloch wavenumber k (k_x, k_y), and the coefficient of the cubic term are treated as the second and third continuation parameters, respectively. Then we compute the Bloch bands/surfaces for the 1D/2D problem with linear counterparts. At the second stage we use μ and k/k_x or k_y as the continuation parameters simultaneously with two constraint conditions. The states without linear counterparts in the GPE can be obtained via states with linear counterparts. Numerical results are reported for both 1D and 2D problems.

1. Introduction

Superflow of Bose–Einstein condensates (BEC) [1,2] in an optical lattice is represented by a Bloch wave, which can be regarded as a plane wave modulated by the periodic potential. When the number of dilute atoms or molecules is large, the BEC system is well described by the mean-field theory, and is governed by the well-known Gross–Pitaevskii equation (GPE) [3,4]:

$$\mathbf{i}\hbar\frac{\partial\Psi}{\partial t} = -\frac{\hbar^2}{2m}\Delta\Psi + V(x)\Psi + \frac{4\pi\hbar^2 a_s}{m}|\Psi|^2\Psi, \tag{1.1}$$

where m is the atomic mass, a_s the s-wave scattering length, and $V(x)$ the external potential imposed on the physical system. We consider the potential as the optical lattices created either by two (1D) or four (2D) laser beams, i.e.,

$$V(x) = V_0\cos 2k_L x \quad \text{or} \quad V(\mathbf{x}) = V_0(\cos 2k_{Lx}x + \cos 2k_{Ly}y),$$
$$\mathbf{x} = (x, y), \tag{1.2}$$

respectively, where V_0 is a constant which is proportional to the laser intensity, and k_L (respectively, k_{Lx} and k_{Ly} in the x- and y-coordinate) is the wavenumber of the laser [5]. Eq. (1.1) is also known as the nonlinear Schrödinger equation (NLS).

For simplicity we consider the dimensionless 1D GPE of the following form

$$\mathbf{i}\frac{\partial\Psi}{\partial t} = -\frac{1}{2}\Delta\Psi + \nu\cos x\cdot\Psi + c|\Psi|^2\Psi, \tag{1.3}$$

where all the variables are scaled to be dimensionless with the system's basic parameters: the coefficient of the periodic potential ν is in units of $\frac{4\hbar^2k^2}{m}$, the wave function Ψ in units of $\sqrt{n_0}$, where n_0 is the averaged BEC density, the time variable t in units of $\frac{m}{4\hbar^2k^2}$, the spatial variable x in units of $\frac{1}{2k}$, and the coupling constant $c = \frac{\pi n_0 a_s}{k^2}$. Here and in what follows, we have omitted the capital subscript L in the wavenumber. Substituting the formula

$$\Psi(x,t) = e^{-\mathbf{i}\mu t}\psi(x) \tag{1.4}$$

into (1.3), we obtain the nonlinear eigenvalue problem

$$-\frac{1}{2}\Delta\psi + \nu\cos x\cdot\psi + c|\psi^2|\psi = \mu\psi, \tag{1.5}$$

where μ is the chemical potential, and $\psi(x)$ is a complex stationary state wave function. The energy functional associated with (1.5) is

* Corresponding author.
E-mail addresses: cschien@amath.nchu.edu.tw (C.-S. Chien), slchang@mail.stut.edu.tw (S.-L. Chang), wubiao@pku.edu.cn (B. Wu).

[1] Supported by the National Science Council of ROC (Taiwan) through Project NSC 98-2115-M231-001-MY3.

0010-4655/$ – see front matter © 2010 Elsevier B.V. All rights reserved.
doi:10.1016/j.cpc.2010.06.030

$$E_\mu(\psi) = \int_\Omega \left[\left(-\frac{1}{2}\Delta + \nu\cos x\right)\psi\cdot\psi^* + \frac{c}{2}|\psi|^4 - \mu|\psi|^2\right]dx,$$
$$\Omega = [0, 2\pi], \tag{1.6}$$

where ψ^* denotes the complex conjugate of the wave function ψ. Any nontrivial solution of (1.5) which minimizes the energy functional (1.6) is called a nonlinear eigenstate [5] or nonlinear coherent mode [6] associated with the nonlinear eigenvalue μ. Bloch waves are nonlinear eigenstates of the form

$$\psi(x) = e^{\mathbf{i}kx}\phi_k(x), \tag{1.7}$$

where $\phi_k(x)$ is a complex periodic function of period 2π and k the Bloch wavenumber. Substituting (1.7) into (1.5), we obtain the following equation for each Bloch wave state ϕ_k:

$$-\frac{1}{2}(\nabla + \mathbf{i}k)^2\phi_k + \nu\cos x\cdot\phi_k + c|\phi_k|^2\phi_k = \mu\phi_k,$$
$$\phi_k(x+2\pi) = \phi_k(x), \quad x\in\Omega, \tag{1.8}$$

with constraint

$$\int |\phi_k(x)|^2\,dx = \nu_\Omega = 2\pi, \tag{1.9}$$

where ν_Ω denotes the volume of Ω. In (1.8) the nonlinear eigenvalue μ can be regarded as a function of k, i.e., $\mu = \mu(k)$ for states with linear counterparts. The set of eigenvalues $\mu(k)$ are called Bloch bands.

During the past decade various approaches have been used to find the Bloch waves ϕ_k in 1D. At the beginning, Wu and Niu [7] used a two-mode approximation method to find the Bloch states near the edge of the Brillouin zone and discovered a loop structure in the Bloch band. Later Wu and Niu [8] used Fourier series to expand ϕ_k and found the Bloch waves by minimizing the energy functional. However, this method could not reproduce the loop structure. Diakonov et al. [9] recovered this loop structure by solving (1.8) for different values of μ and k, and obtained the Bloch bands $\mu(k)$ by interpolation. In [5] Wu and Niu reproduced the results of Diakonov et al. [9] with a new method. They expanded ϕ_k using a finite sum of Fourier series

$$\phi_k(x) = \sum_{n=-N}^{N} a_n e^{\mathbf{i}nx}, \quad N\in\mathbf{N}, \tag{1.10}$$

and substituted (1.10) into (1.8) to obtain a nonlinear system of $2N+1$ equations in $2N+2$ unknowns $f_n(a_0, a_{\pm1}, \ldots, a_{\pm N}, \mu) = 0$. The Bloch wave was obtained by minimizing

$$S = \sum_{n=-N}^{N} f_n^2$$

under the constraint $\sum_{n=-N}^{N}|a_n|^2 = 2\pi$. All the numerical methods mentioned above are efficient to handle the 1D problem but seem to have difficulties with the 2D problem. To the best of our knowledge, the 2D problem has never been completely solved in physics literatures.

Recently, a numerical continuation algorithm, namely, AUTO97 [10], has been used to investigate traveling waves in saturable nonlinear Schrödinger lattices [11]. On the other hand, Chang, Chien and Jeng [12], and Chang and Chien [13] have studied efficient continuation algorithms for nonlinear Schrödinger equations. In this paper, we present novel two-stage continuation algorithms for computing Bloch bands/surfaces of the GPE in 1D/2D. Starting with the 1D problem, we split the complex function $\phi_k(x)$ in (1.8) into the sum of its real part and imaginary part. Then (1.8) becomes a system of two real nonlinear eigenvalue problems. We may discretize the system by using finite differences, finite elements or pseudo-spectral methods. In either case we obtain a nonlinear system of equations involving multiparameters. At the first stage, we use an efficient Taylor predictor–Newton corrector continuation algorithm [14] to trace the ground state solution curves. The parameters μ, k, and c in (1.8) are treated as the continuation parameters. For the 2D problem we have one additional continuation parameter k_y. Thus the eigenvalue μ depends on k_x and k_y, and the Bloch bands will be replaced by the Bloch surfaces. For the 1D problem the constraint (1.9) is regarded as a target point on the ground state solution curve for each curve-tracking. We stop the curve-tracking whenever the target point is reached. Then we obtain nonlinear eigenstates of (1.8) with linear counterparts. However, there are nonlinear Bloch waves which do not have their linear counterparts [5,15–17]. This is the case where a loop structure can occur for $c > \nu$.

At the second stage we compute the closed loops in the Bloch bands where the effect of nonlinearity is increasing. We treat μ and k as the continuation parameters simultaneously. Starting with the first bifurcation point on the trivial solution curve of (1.8) for $k = \pm 0.5$, and say, $c = 0.2$, we follow the solution curve using the first stage continuation algorithm until the target point is reached. The target points located at the cusp points of the band consist of two nonlinear eigenstates with and without linear counterparts. We then switch from the first stage to the second stage continuation algorithm, and implement the second order Taylor predictor on the parameter k. Next we perform the Newton corrector to compute (ϕ_k, μ, k) where (1.9) is used as the second constraint for the augmented linear system in addition to the unit tangent vector used in the first stage. We proceed in this way until the closed loop is obtained. Thus the eigenstate without linear counterpart can be obtained indirectly from the Schrödinger eigenvalue problem (SEP) by passing through the state with linear counterpart. The two-stage continuation algorithm for the 1D problem can be modified to compute the Bloch surfaces of the 2D problem.

This paper is organized as follows. In Section 2 we briefly review the relationship among eigenvalues, energy levels and bifurcations of the GPE. In particular, we show how an eigenpair of the linear eigenvalue problem associated with the GPE can be used as an initial guess for computing its nonlinear counterpart using continuation methods. In Section 3 we derive the nonlinear eigenstate without linear counterpart for the 1D problem (1.8) with constraint (1.9) at $k = \frac{1}{2}$, where the closed loop of the Bloch band occurs. In Section 4 we describe two-stage continuation algorithms for computing the lowest Bloch bands and surfaces in 1D and 2D, respectively. Our numerical results for the 1D and 2D problems are reported in Section 5. Finally, some concluding remarks are given in Section 6.

2. Nonlinear eigenstates with linear counterparts

For completeness we briefly discuss how the eigenpairs of the Schrödinger eigenvalue problem or the linear Schrödinger equation may be exploited to compute their nonlinear counterparts of the NLS. In [12,13] we used continuation methods to study the ground state and excited-state solutions of the following NLS:

$$\mathbf{i}\frac{\partial}{\partial t}\Psi(\mathbf{x},t) = -\frac{1}{2}\Delta\Psi + V(\mathbf{x})\Psi + c|\Psi|^2\Psi, \quad t>0,$$
$$\mathbf{x} = (x,y)\in\Omega, \tag{2.1}$$

where $\Psi = \Psi(\mathbf{x},t)$ is the macroscopic wave function of the BEC, $V(\mathbf{x}) = \frac{1}{2}(\gamma_x^2x^2 + \gamma_y^2y^2)$ the magnetic trapping potential with γ_x and γ_y the trap frequencies in x- and y-direction, the constant c can be positive or negative, and $\Omega\subset\mathbf{R}^2$ a bounded domain with piecewise smooth boundary $\partial\Omega$. Eq. (2.1) can be easily generalized to M-component NLS, $M\geqslant 2$.

An important invariant of the NLS is the mass conservation constraint, or the normalization of the wave function

$$\int_{\Omega} \left|\Psi(\mathbf{x},t)\right|^2 d\mathbf{x} = 1, \quad t \geqslant 0, \tag{2.2}$$

which means that the total probability of finding the particle anywhere in Ω must be 1.

Substituting the formula

$$\Psi(\mathbf{x},t) = e^{-\mathbf{i}\mu t} u(\mathbf{x}) \tag{2.3}$$

into (2.1), we obtain the stationary state nonlinear eigenvalue problem

$$F(u,\mu) = -\frac{1}{2}\Delta u - \mu u + V(\mathbf{x})u + cu^3 = 0 \quad \text{in } \Omega, \tag{2.4}$$

where μ is the chemical potential which is proportional to the total energy of the system, and $u(\mathbf{x})$ a real function independent of t. To compute an energy level of (2.4) using numerical continuation methods, we have to trace the corresponding solution curve branching from a bifurcation point on the trivial solution curve $\{(u,\mu) = (0,\mu) \mid \mu \in \mathbf{R}\}$. Here the chemical potential μ is treated as the continuation parameter [12,13]. We stop the curve-tracking whenever the mass conservation constraint for the stationary state wave function

$$\int_{\Omega} \left|u(\mathbf{x})\right|^2 dx = \|u\|_2 = 1 \tag{2.5}$$

is satisfied for some wave function $\tilde{u}$ and chemical value $\tilde{\lambda}$. We denote $(\tilde{u},\tilde{\lambda})$ as a target point in the curve-tracking. Note that the parameter of a bifurcation point of the GPE (NLS) is just an eigenvalue of the associated Schrödinger eigenvalue problem (SEP)

$$-\frac{1}{2}\Delta u + V(\mathbf{x})u = \mu u \quad \text{in } \Omega, \tag{2.6}$$

We may detect bifurcation points along the trivial solution curve of (2.4) by monitoring the singularity of the Jacobian matrix DF. However, the computational cost can be very expensive if the order of DF is large. To reduce the computational cost we may compute the first few eigenpairs of (2.4) using the Jacobi–Davidson method or some well-known codes. The procedure discussed above shows that continuation can compute states of the NLS with linear counterparts. In particular, it can be applied to compute Bloch waves of (1.8).

Recently, we have compared the performance of a variant of the simplified two-grid continuation algorithm [13] with the imaginary time evolution method (ITEM), and some variants of the ITEM, such as AITEM and AITEM (A.N.) [18]. We refer to [19] for the details.

3. An eigenstate without linear counterpart

We now present an analytical Bloch wave solution of the GPE, which has no linear counterpart. This example illustrates the difficulty to find Bloch waves for the GPE. We rewrite the time-independent 1D GPE (1.5) as

$$-\frac{1}{2}\frac{d^2\psi}{dx^2} + c|\psi|^2\psi + \nu\cos x\cdot\psi = \mu\psi, \quad x \in \Omega = [0,2\pi], \tag{3.1}$$

with constraint

$$\int_{\Omega} \left|\psi(x)\right|^2 dx = 2\pi. \tag{3.2}$$

In [5] Wu and Niu used $\psi(x) = e^{\mathbf{i}kx}\phi_k(x) = ae^{\mathbf{i}kx} + be^{-\mathbf{i}kx}$, $a,b \in \mathbf{R}$, to derive the eigenstate of (3.1) without linear counterpart. To be precise, let

$$\psi(x) = e^{\mathbf{i}kx}\phi_k(x) = ae^{\mathbf{i}kx} + be^{-\mathbf{i}kx}, \quad a,b \in \mathbf{R}. \tag{3.3}$$

We have

$$\psi_x = k\mathbf{i}\left(ae^{\mathbf{i}kx} - be^{-\mathbf{i}kx}\right), \qquad \psi_{xx} = -k^2\psi, \tag{3.4a}$$

and

$$|\psi|^2 = \left(a^2+b^2\right) + 2ab\left(\cos^2 kx - \sin^2 kx\right). \tag{3.4b}$$

Substituting (3.4a) and (3.4b) into (3.1), we obtain

$$\begin{aligned}&\frac{1}{2}k^2\psi + c\left[\left(a^2+b^2\right) + 2ab\left(\cos^2 kx - \sin^2 kx\right)\right]\psi + \nu\cos x\cdot\psi \\ &\quad = \left[\frac{1}{2}k^2 + c\left(a^2+b^2\right) + 2abc\cos(2kx) + \nu\cos x\right]\psi \\ &\quad = \mu(k)\psi,\end{aligned} \tag{3.5}$$

where $\mu(k) = \frac{k^2}{2} + c(a^2+b^2) + 2abc\cos(2kx) + \nu\cos x$. For $k = \frac{1}{2}$, we have

$$\mu\left(\frac{1}{2}\right) = \frac{1}{8} + c\left(a^2+b^2\right) + (\nu + 2abc)\cos x.$$

Let $\nu = -2abc$. Then

$$2ab = -\frac{\nu}{c}. \tag{3.6}$$

From the mass conservation constraint, for $k = \frac{1}{2}$ we have

$$\begin{aligned}\int_{\Omega} \left|\psi(x)\right|^2 dx &= \int_0^{2\pi} \left[\left(a^2+b^2\right) + 2ab\cos(2kx)\right] dx \\ &= 2\pi\left(a^2+b^2\right).\end{aligned} \tag{3.7}$$

If we choose

$$a^2 + b^2 = 1 \tag{3.8}$$

in (3.7), then we obtain the constraint (3.2), and hence Eq. (3.4) in [5]. To be precise, we add (3.6) and (3.8) together, and obtain

$$(a+b)^2 = 1 - \frac{\nu}{c},$$

or

$$a + b = \pm\sqrt{1 - \frac{\nu}{c}} = \pm\frac{\sqrt{c-\nu}}{\sqrt{c}}.$$

Subtracting (3.8) from (3.6), we have

$$(a-b)^2 = 1 + \frac{\nu}{c},$$

or

$$a - b = \pm\sqrt{1 + \frac{\nu}{c}} = \pm\frac{\sqrt{c+\nu}}{\sqrt{c}}.$$

So we obtain two solutions for a and b as follows:

$$a = \frac{\sqrt{c-\nu} + \sqrt{c+\nu}}{2\sqrt{c}}, \qquad b = \frac{\sqrt{c-\nu} - \sqrt{c+\nu}}{2\sqrt{c}}, \tag{3.9a}$$

$$a = \frac{\sqrt{c-\nu} - \sqrt{c+\nu}}{2\sqrt{c}}, \qquad b = \frac{\sqrt{c-\nu} + \sqrt{c+\nu}}{2\sqrt{c}} \tag{3.9b}$$

and

$$\mu\left(\frac{1}{2}\right) = \frac{1}{8} + c.$$

Substituting (3.9a) and $k = \frac{1}{2}$ into (3.3), we obtain the nonlinear eigenstate of (1.8), which is the same as Eq. (3.4) in [5]. This Bloch wave solution has no linear counterpart since a and b diverges when c becomes zero.

4. Two-stage continuation algorithms

In this section, we describe two-stage continuation algorithms for computing Bloch bands/surfaces of the 1D/2D problem. The first stage continuation algorithm computes the eigenstates of (1.8) with linear counterparts while the second stage deals with eigenstates without linear counterparts. In the first stage we use the chemical potential μ as the continuation parameter, and the unit tangent vector as the constraint condition. The second stage continuation algorithm is a straightforward extension of the first stage with one additional continuation parameter, namely, the wavenumber k, and one additional constraint condition, namely, (1.9). The algorithm for the 2D problem is a slight modification of that for the 1D problem, and will be discussed independently.

4.1. 1D problem

Let $\phi_k(x) = p(x) + \mathbf{i}q(x)$ in (1.8), where $p(x)$ and $q(x)$ are two real functions. The real part and imaginary part of (1.8) can be expressed as

$$\begin{aligned}
&-\frac{1}{2}p_{xx} + kq_x + \frac{k^2}{2}p + \nu\cos x \cdot p + c\left(p^2+q^2\right)p = \mu p,\\
&-\frac{1}{2}q_{xx} - kp_x + \frac{k^2}{2}q + \nu\cos x \cdot q + c\left(p^2+q^2\right)q = \mu q,\\
&\text{in } \Omega = (0, 2\pi),\\
&p(x) = p(x+2\pi), \quad q(x) = q(x+2\pi), \quad x \in \Omega.
\end{aligned} \tag{4.1}$$

We discretize (4.1) using the centered difference approximations with uniform meshsize $h = \frac{2\pi}{N}$. For simplicity we use P and Q to denote the discrete grid functions $p(x)$ and $q(x)$ on Ω. The centered difference analogue of (4.1) is

$$F(P, Q, \mu, k) = \begin{bmatrix} F_1(P, Q, \mu, k) \\ F_2(P, Q, \mu, k) \end{bmatrix} = 0, \tag{4.2}$$

where

$$\begin{aligned}
F_1(P, Q, \mu, k) &= AP + kBQ - \mu P\\
&\quad + \left(\frac{k^2}{2}I + \nu\cos xI + c(P\circ P + Q\circ Q)\right)\circ P = 0,\\
F_2(P, Q, \mu, k) &= -kBP + AQ - \mu Q\\
&\quad + \left(\frac{k^2}{2}I + \nu\cos xI + c(P\circ P + Q\circ Q)\right)\circ Q = 0,
\end{aligned} \tag{4.3}$$

where "$\circ$" denotes the Hadamard product,

$$A = \frac{1}{2h^2}\begin{bmatrix} 2 & -1 & & & -1 \\ -1 & 2 & \ddots & & \\ & \ddots & \ddots & \ddots & \\ & & \ddots & \ddots & -1 \\ -1 & & & -1 & 2 \end{bmatrix} \in \mathbf{R}^{N\times N},$$

$$B = \frac{1}{2h}\begin{bmatrix} 0 & 1 & & & -1 \\ -1 & 0 & \ddots & & \\ & \ddots & \ddots & \ddots & \\ & & \ddots & \ddots & 1 \\ 1 & & & -1 & 0 \end{bmatrix} \in \mathbf{R}^{N\times N}$$

and the identity matrix $I \in \mathbf{R}^{N\times N}$. Note that B is skew-symmetric, i.e., $B^T = -B$. Let $W = [P, Q]^T$. In the first stage continuation algorithm, for any wavenumber $k \in [-1, 1]$, there is one and only one chemical potential μ associated with k. That is, we have $\mu = \mu(k)$ for $k \in [-1, 1]$. Thus in this stage we can fix k and only treat μ as the continuation parameter. The corresponding Jacobian matrix $DF = [D_W F, D_\mu F]$ is

$$DF = \begin{bmatrix} A - (\mu - \frac{k^2}{2} - \nu\cos x)I \\ \quad + c\,\mathrm{diag}((3P\circ P + Q\circ Q)) & kB + 2c\,\mathrm{diag}(P\circ Q) & -P \\ -kB + 2c\,\mathrm{diag}(P\circ Q) & A - (\mu - \frac{k^2}{2} - \nu\cos x)I \\ & \quad + c\,\mathrm{diag}((P\circ P + 3Q\circ Q)) & -Q \end{bmatrix}. \tag{4.4}$$

Note that $D_W F$ is the linearization of the mapping F at the equilibrium $W_0 = [0, 0]^T$, i.e.,

$$D_W F(W_0, \mu) = K - \mu\begin{bmatrix} I & 0 \\ 0 & I \end{bmatrix}, \tag{4.5}$$

where

$$K = \begin{bmatrix} A + (\frac{k^2}{2} + \nu\cos x)I & kB \\ -kB & A + (\frac{k^2}{2} + \nu\cos x)I \end{bmatrix}. \tag{4.6}$$

Since A is symmetric and B is skew-symmetric, K is a symmetric matrix. We have the following result. The proof can be found in [13] and is omitted here.

Theorem 4.1. *All the eigenvalues of the matrix K are real and at least double.*

4.2. Taylor predictor and Newton corrector

The nonlinear system (4.2) can be simplified as

$$F(y) = 0, \tag{4.7}$$

where in the first stage continuation algorithm $F : \mathbf{R}^{2N+1} \to \mathbf{R}^{2N}$ is a sufficiently smooth mapping with $y = (P, Q, \mu)$. In the second stage continuation algorithm we will treat both μ and k as the continuation parameters simultaneously. Therefore the smooth mapping should be defined as $F : \mathbf{R}^{2N+2} \to \mathbf{R}^{2N}$ with $y = (P, Q, \mu, k)$. For convenience we consider the first stage continuation algorithm at this moment. Let $y^{(k)}$ be an approximating point on some solution curve Γ of (4.7). We choose a parameterizing equation

$$N_k(y, \tau) = 0, \tag{4.8}$$

where $N_k : \mathbf{R}^{2N+1} \times \mathbf{R} \to \mathbf{R}^{2N+1}$ is a sufficiently smooth mapping such that the inflated nonlinear system.

$$\begin{aligned}
&T_k(y, \tau) := \begin{bmatrix} F(y) \\ N_k(y, \tau) \end{bmatrix} = 0,\\
&T_k : \mathbf{R}^{2N+1} \times \mathbf{R} \to \mathbf{R}^{2N+1},
\end{aligned} \tag{4.9}$$

is locally uniquely solvable in a neighborhood of $(y, \tau) = (y^{(k)}, 0)$. Here τ denotes the local parameter defined in (4.8). If $|\tau|$ is sufficiently small, the solution function $y^{(k)}(\tau)$ of (4.9) defines a local parametrization of the solution curve Γ.

The Taylor expansion of $y^{(k)}(\tau)$ is

$$y^{(k)}(\tau) = y^{(k)}(0) + \tau\,\dot{y}^{(k)}(0) + \frac{\tau^2}{2}\ddot{y}^{(k)}(0) + \frac{\tau^3}{6}\dddot{y}^{(k)}(0) + O(\tau^4).$$

Schwetlick and Cleve [14] proposed the second/third Taylor predictor for curve-tracking, where the directional derivatives containing $\ddot{F}$ and $\dddot{F}$ could be efficiently approximated by a few function evaluations. The numerical results in [14] show that the Taylor predictors can reduce the computational cost. More precisely, the number of calculated approximating points and the number of evaluations and factorizations of Jacobian matrices are less than the general predictor–corrector methods known from literature.

To find the Bloch waves of (1.8) with linear counterparts, we will implement the second order Taylor predictor–Newton corrector in the context of the simplified two-grid continuation algorithm for computing the ground state solutions $\{(\phi_k, \mu)\}$ of (4.1). Here the chemical potential μ is treated as the continuation parameter [12,13]. The other two parameters c and $k \in [-1, 1]$ are keep fixed for each curve-tracking.

Note that the Bloch waves are symmetric with respect to $k = 0$. To save unnecessary computations we may consider $k \in [0, 0.5]$. To be consistent with the data used in [5], we choose the coefficient of the periodic potential $\nu = 0.1$. The constraint (1.9) is regarded as a target point on each nontrivial solution curve. Whenever the target point is reached, we also obtain the energy level μ. To start with, we set $c = k = 0$ and trace the ground state solution of (4.1) until the target point is reached. Here we treat k as the second continuation parameter with step-size $s_1 = 0.05$. Next, we trace the ground state solution of (4.1) with $c = 0$ and $k = 0.05$. We proceed in this way until the ground state solution of (4.1) with $c = 0$ and $k = 0.5$ is traced. Then we obtain the first Bloch wave for the linear problem with $c = 0$. Now we treat the third continuation parameter $c = 0.05$, and trace the ground state solution of (4.1) with $k = 0$. We repeat the same process as above until the ground state solution associated with $c = 0.05$ and $k = 0.5$ is obtained. We continue this procedure until the ground state solution of (4.1) with $c = 0.2$ and $k = 0.5$ is traced.

Suppose that $(W^{(j)}, \mu^{(j)}) = (P^{(j)}, Q^{(j)}, \mu^{(j)})$ is an accepted approximating point on the solution curve in the jth continuation step. Then we use the second order Taylor predictor to predict a new point $(W^{(j+1,1)}, \mu^{(j+1,1)})$, which will be used as an initial guess for the Newton corrector. We perform the Newton corrector until it converges to the desired approximating point $(W^{(j+1)}, \mu^{(j+1)})$.

Algorithm 4.2. The first stage continuation for the Bloch bands with linear counterparts.

Input:

μ := the chemical potential which is used as the first continuation parameter.
k := the second continuation parameter, $k \in [0, 0.5]$ with stepsize $s_1 = 0.05$.
c := the third continuation parameter, $c \in [0, 0.2]$ with stepsize $s_2 = 0.05$.
ε := accuracy tolerance for the Newton corrector on the coarse grid and fine grid.
Initialization: $c = k = 0$.

Step 1. Use a modification of the simplified two-grid scheme [13] to compute the ground state solution of (4.1) with constraint (1.9), and obtain the energy level $\mu(k)$ for c.
  (a) Outer continuation. Use the Taylor predictor–Newton corrector continuation algorithm to compute approximating points on the coarse grid until the target point is reached where $\|F\| < \varepsilon$.
  (b) Compute the target point on the fine grid.
    (i) Predictor: Use the target point obtained in (a) as the predicted point.
    (ii) Make a correction on the fine grid by solving the linear approximation of $F(W, \mu) = 0$.
    (iii) Use the corrected point as an initial guess, and perform the Newton corrector until the target point on the fine grid is reached.

Step 2. Set $k = k + s_1$.
  If $k \leqslant 0.5$, go to Step 1.
  Else if $k > 0.5$, set $k = 0$, and $c = c + s_2$.
    If $c < 0.2$, go to Step 1.
    Else if $c = 0.2$, stop.
    End if
  End if

As we may see from Fig. 1 in [5], there exist two eigenstates at the cusp points of the Bloch wave where $c = 0.2$ and $k = \pm 0.5$. One of them has linear counterpart, and the other does not have linear counterpart. At the second stage of the continuation algorithm, we will show how the eigenstate without linear counterpart may be obtained using the information of the SEP. To start with, we choose $c = 0.2$ and $k = 0.5$. Then we use the first stage continuation algorithm to trace the solution curve of (4.1) branching from the first bifurcation $(p, q, \mu^*) = (0, 0, \mu^*)$, where μ^* is the minimum eigenvalue of the linear eigenvalue problem associated with (4.1). We stop the curve-tracking whenever the target point is reached. Note that at the target point both eigenstates with/without linear counterparts have the same values in the domain Ω. Denote the target point by $Z^{(0)} = (W, \mu^*, 0.5)$, where $W = (P, Q)$. Now we wish to compute the closed loops in some neighborhoods of $k = \pm 0.5$. Note that for any wavenumber k in these neighborhoods, the corresponding chemical potential is not unique. Therefore the parameters μ and k must be treated as the continuation parameters simultaneously, where the corresponding nonlinear mapping is given by $F : \mathbf{R}^{2N+2} \to \mathbf{R}^{2N}$. In addition to using the unit tangent vector as the first constraint condition, we also need to use the mass conservation constraint (1.9) as the second constraint condition. We express the discrete analogue of (1.9) as

$$F_3(P, Q, \mu, k) = -\frac{1}{2}\left(P^T \cdot P + Q^T \cdot Q\right) + \frac{\pi}{h} = 0, \tag{4.10}$$

and perform the Taylor predictor with k as the continuation parameter and with stepsize τ. The Fréchet derivative of F is denoted by $DF = [D_{(W,\mu)}F, D_k F] \in \mathbf{R}^{2N\times(2N+2)}$, where the principal $2N \times 2N$ submatrix is just $D_W F$ in (4.4). Note that $D_k F = [BQ + kP, -BP + kQ]^T$. Now we add the unit tangent vector

$$\mathbf{v} := \frac{[\dot{W}, \dot{\mu}, 0]}{\|[\dot{W}, \dot{\mu}, 0]\|}$$

obtained in the previous continuation step, and $DF_3 = [-P\ -Q\ 0\ 0]$ as the last two rows for DF, and obtain the augmented Jacobian matrix

$$H = \begin{bmatrix} DF \\ DF_3 \\ \mathbf{v}^T \end{bmatrix} \in \mathbf{R}^{(2N+2)\times(2N+2)}. \tag{4.11}$$

Subsequently we perform the Newton corrector

$$H \begin{bmatrix} \delta W \\ \delta\mu \\ \delta k \end{bmatrix} = \begin{bmatrix} -F(S^{(1)}) \\ -F_3(S^{(1)}) \\ 0 \end{bmatrix}, \tag{4.12}$$

where the predicted point $S^{(1)}$ is used as an initial guess and the unknown vector $[\delta W, \delta\mu, \delta k]^T$ denotes the increment on each

component. If the Newton iterates converge to an approximate solution $Z^{(1)}$ of F, then we go to the next continuation step and perform the second order Taylor predictor as above. Note that the value of k will be changed in the corrector. We repeat the process mentioned above until the closed loop is obtained.

Algorithm 4.3. The second stage continuation for the closed loops.

Input:
$\tau :=$ step size in the second order Taylor predictor.
$c := 0.2, \quad \nu := 0.1, \quad k := 0.5.$

Step 1. Use Algorithm 4.2 to compute the ground state solution $Z^{(0)} = (W, \mu^*, 0.5)$ of (4.1).
Step 2. (i) Treat both μ and k as the continuation parameter simultaneously.
(ii) Use the second order Taylor predictor to obtain the predicted point $S^{(1)}$.
(iii) Newton corrector. Solve (4.12) until convergence, and obtain the approximate solution $Z^{(1)}$.
Step 3. If the closed loop is not obtained, then set $Z^{(0)} := Z^{(1)}$ and go to Step 1.
Else
stop.
End if

4.3. 2D problem

We consider the 2D nonlinear eigenvalue problem in a periodic potential

$$-\frac{1}{2}\Delta\psi(\mathbf{x}) + \nu[\cos x + \cos y]\psi(\mathbf{x}) + c\left|\psi(\mathbf{x})\right|^2\psi(\mathbf{x}) = \mu\psi(\mathbf{x}),$$
$$\Omega = (0, 2\pi)^2, \qquad c \in [0, 0.3],$$
$$\psi(x, y) = \psi(x + 2\pi, y) = \psi(x, y + 2\pi),$$
$$\mathbf{x} = (x, y) \in \Omega, \tag{4.13}$$

with constraint

$$\int_\Omega \left|\psi(\mathbf{x})\right|^2 d\mathbf{x} = \nu_\Omega = 4\pi^2. \tag{4.14}$$

Eq. (4.13) has the following Bloch wave solutions

$$\psi(\mathbf{x}) = e^{\mathbf{i}\mathbf{k}\cdot\mathbf{x}}\phi_{\mathbf{k}}(\mathbf{x}), \tag{4.15}$$

where $\phi_{\mathbf{k}}(x, y)$ satisfies

$$\phi_{\mathbf{k}}(x, y) = \phi_{\mathbf{k}}(x + 2\pi, y) = \phi_{\mathbf{k}}(x, y + 2\pi) \tag{4.16}$$

and $\mathbf{k} = (k_x, k_y)$ is the Bloch wave vector with $k_x, k_y \in [-\frac{1}{2}, \frac{1}{2}]$. Similar to the derivation of (1.8), we have

$$-\frac{1}{2}(\nabla + \mathbf{i}\mathbf{k})^2\phi_{\mathbf{k}}(\mathbf{x}) + \nu[\cos x + \cos y]\phi_{\mathbf{k}}(\mathbf{x}) + c\left|\phi_{\mathbf{k}}(\mathbf{x})\right|^2\phi_{\mathbf{k}}(\mathbf{x}) = \mu\phi_{\mathbf{k}}(\mathbf{x}), \quad \mathbf{x} \in \Omega, \tag{4.17}$$

where $\phi_{\mathbf{k}}(\mathbf{x})$ is a complex function. Similar to the discussions in Section 4.1, let

$$\phi_{\mathbf{k}}(\mathbf{x}) = p(\mathbf{x}) + \mathbf{i}q(\mathbf{x}), \tag{4.18}$$

where $p(\mathbf{x})$ and $q(\mathbf{x})$ are two real functions. The real part and imaginary part of (4.17) can be expressed as

$$-\frac{1}{2}\Delta p + (k_x \cdot q_x + k_y \cdot q_y) + \frac{1}{2}\left(k_x^2 + k_y^2\right)p + \nu(\cos x + \cos y)p + c\left(p^2 + q^2\right)p = \mu p,$$
$$-\frac{1}{2}\Delta q - (k_x \cdot p_x + k_y \cdot p_y) + \frac{1}{2}\left(k_x^2 + k_y^2\right)q + \nu(\cos x + \cos y)q + c\left(p^2 + q^2\right)q = \mu q, \quad \text{in } \Omega,$$
$$p(x, y) = p(x + 2\pi, y) = p(x, y + 2\pi),$$
$$q(x, y) = q(x + 2\pi, y) = q(x, y + 2\pi), \quad (x, y) \in \Omega. \tag{4.19}$$

As we may see from (4.19) that the eigenvalue μ depends on the wavenumbers k_x and k_y. That is, $\mu = \mu(k_x, k_y)$ is a function of two variables. Thus the Bloch bands for the 1D problem will be replaced by the Bloch surfaces for the 2D problem. Now Algorithm 4.2 can be modified to compute the Bloch surfaces for the 2D problem with linear counterparts except that we have four continuation parameters μ, k_x, k_y, c, where $k_x, k_y \in [-0.5, 0.5]$. To compute the two closed loops for the Bloch surface at $k_x = k_y = 0.5$, we rewrite the discrete formulation of the first two equations in (4.19) as

$$\hat{F}_1(P, Q, \mu, k_x, k_y) = 0, \qquad \hat{F}_2(P, Q, \mu, k_x, k_y) = 0. \tag{4.20}$$

Note that compared to (4.2) we have one additional parameter. However, the constraint conditions for the 2D and 1D problems are the same. The difficulty can be easily overcome by fixing one of the wavenumber, say at $k_y = 0.5$, and treating μ and k_x as the continuation parameters simultaneously. Thus (4.20) can be solved using analogous algorithms for the 1D problem. Similarly we may obtain another closed loop by fixing $k_x = 0.5$ and treating μ and k_y as the continuation parameters simultaneously. The closed loops at the other three corners of the Bloch surface with $c = 0.3$ can be obtained in a similar way. To compute eigenstates without linear counterparts at one of the four edges of the Bloch vectors, say $k_y = 0.5$, $k_x \in [-0.5, 0.5]$, we treat k_x as the continuation parameter. Then Algorithm 4.3 can be modified to compute closed loops at the edge $k_y = 0.5$. Closed loops at the other edges could be obtained in a similar way.

5. Numerical results

Algorithms 4.2 and 4.3 were implemented to compute the Bloch bands and Bloch surfaces of the GPE in 1D and 2D. The accuracy tolerance for the Newton corrector is 10^{-8}. All computations were executed on a Pentium 4 PC using MATLAB language.

Example 1 *(1D problem).* We discretized (4.1) using the centered difference approximation with uniform meshsize $h = 0.01$ in $\Omega = (0, 2\pi)$. Algorithm 4.2 was implemented to compute the eigenstates of (1.8) with linear counterparts, and obtained the Bloch bands without closed loops. Next, we applied Algorithm 4.3 to compute the closed loops at $k = \pm 0.5$. Fig. 1 shows the lowest Bloch bands of (1.8). The result is exactly the same as Fig. 1 in [5]. Fig. 2 displays the contours of the real part and imaginary part of ϕ_k at the target point with $\nu = 0.1$, $c = 0.2$, $k = 0.5$ and $\mu \approx 0.3249981$. Fig. 3 shows the Bloch wave of (4.1) near the closed loop at $k = 0.5$. The lower curve and the upper one are obtained by the first stage and the second stage continuation, respectively.

Example 2 *(2D problem).* We discretized (4.19) using the centered difference approximations with uniform meshsize $h = \frac{2\pi}{48}$. First we applied the modification of Algorithm 4.2 to compute the eigenstates of (4.19) with linear counterparts. Then we exploited the modification of Algorithm 4.3 to compute the closed loops at the four corners $(k_x, k_y) = (\pm 0.5, \pm 0.5)$ and the four

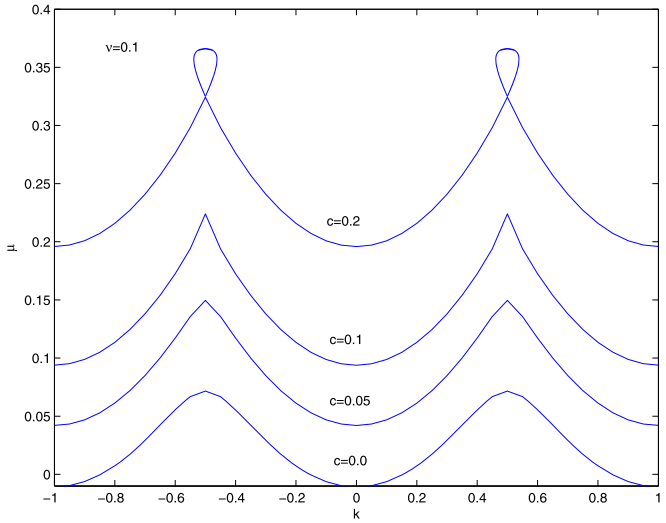

Fig. 1. Lowest Bloch bands at $\nu = 0.1$ for $c = 0.0, 0.05, 0.1$ and 0.2.

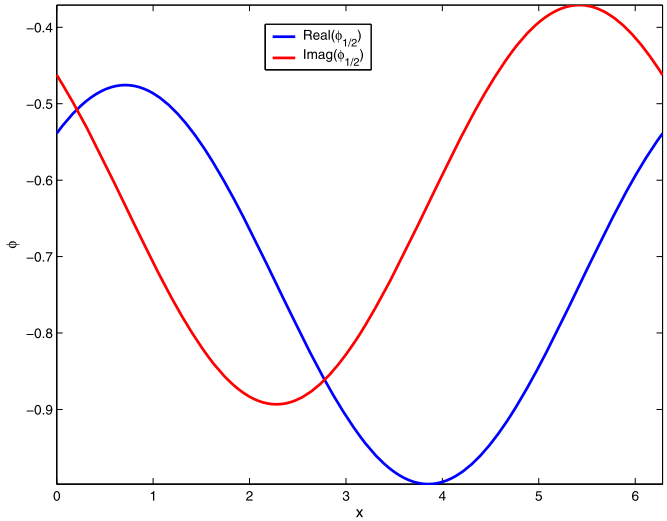

Fig. 2. The curves of the real and imaginary parts of ϕ at the target point with $\nu = 0.1$, $c = 0.2$, $k = 0.5$ and $\mu \approx 0.3249981$.

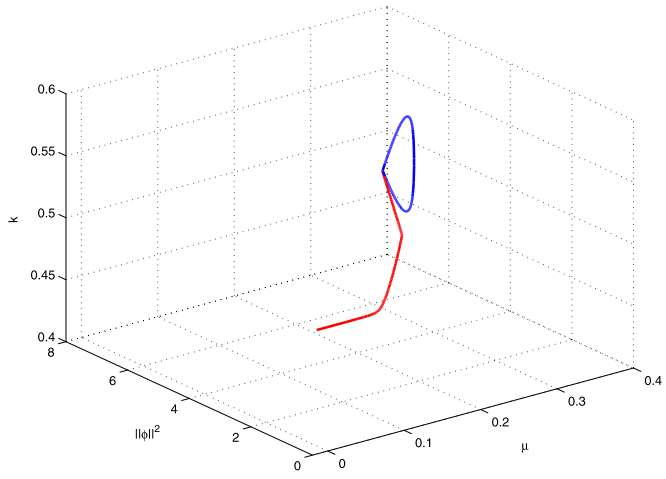

Fig. 3. The Bloch wave of (4.1) represented by the 3D contour near the closed loop where $\nu = 0.1$ and $c = 0.2$. The lower curve and upper curve are obtained by the first stage and second stage continuation, respectively.

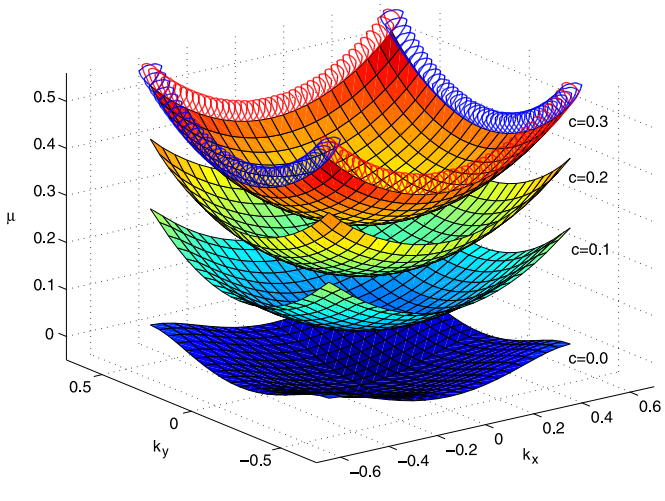

Fig. 4. The Bloch surfaces with $\nu = 0.2$.

edges $k_x = \pm 0.5$, $k_y = \pm 0.5$. That is, we computed the eigenstates of (4.19) without linear counterparts. Fig. 4 shows that the Bloch surfaces are getting sharper at the four corners $(k_x, k_y) = (\pm 0.5, \pm 0.5)$ as c increases from 0 to 0.3. Moreover, the four edges of the Bloch vector $\mathbf{k}$ are surrounded by closed tubes. In particular, at the four corners $(k_x, k_y) = (\pm 0.5, \pm 0.5)$ there are two closed loops. Fig. 5 displays the contours of the real part and imaginary part of $\phi_{\mathbf{k}}$, and $|\phi_{\mathbf{k}}|^2$ with linear counterparts at the target points with $\nu = 0.2$, $\mathbf{k} = (k_x, k_y) = (0, 0.5)$ where $c = 0$ and 0.3. Fig. 6 shows the contours of the real part and imaginary part of $\phi_{\mathbf{k}}$ and $|\phi_{\mathbf{k}}|^2$ with linear counterparts at the target points with $\nu = 0.2$, $\mathbf{k} = (0.5, 0.5)$, and $c = 0$, $\mu \approx 0.0326021$ (left), and $c = 0.3$, $\mu \approx 0.5412584$ (right). Fig. 7 shows the contours of the real part and imaginary part of $\phi_{\mathbf{k}}$ and $|\phi_{\mathbf{k}}|^2$ without linear counterparts at the target points with $\nu = 0.2$, $\mathbf{k} = (0.5, 0.5)$, and $c = 0$, $\mu \approx 0.0326021$ (left), and $c = 0.3$, $\mu \approx 0.5412584$ (right).

6. Conclusions

We have proposed two-stage Taylor predictor–Newton corrector continuation algorithms for computing Bloch bands and Bloch surfaces of 1D and 2D BEC in optical lattices. At the first stage continuation algorithm the eigenpairs of the linear Schrödinger equation have been used as initial guesses for computing their linear counterparts. At the second stage continuation algorithm both Algorithms 4.2 and 4.3 have been implemented to compute eigenstates without linear counterparts. In other words, we also need the information of the SEP and the eigenstates of the GPE with linear counterparts to compute eigenstates without linear counterparts.

References

[1] M.H. Anderson, J.R. Ensher, M.R. Matthews, C.E. Wieman, E.A. Cornell, Observation of Bose–Einstein condensation in a dilute atomic vapor, Science 269 (1995) 198.
[2] K.B. Davis, M.-O. Mewes, M.R. Anderws, N.J. Van Druten, D.S. Durfee, D.M. Kurn, W. Ketterle, Bose–Einstein condensation in a gas of sodium atoms, Phys. Rev. Lett. 75 (1995) 3969.
[3] E.P. Gross, Hydrodynamics of a superfluid condensate, J. Math. Phys. 4 (1963) 195.
[4] L.P. Pitaevskii, Vortex lines in an imperfect Bose gas, Zh. Eksp. Teor. Fiz. 40 (1961) 646.
[5] B. Wu, Q. Niu, Superfluidity of Bose–Einstein condensate in an optical lattice: Landau–Zener tunneling and dynamical instability, New J. Phys. 5 (104) (2003) 1.

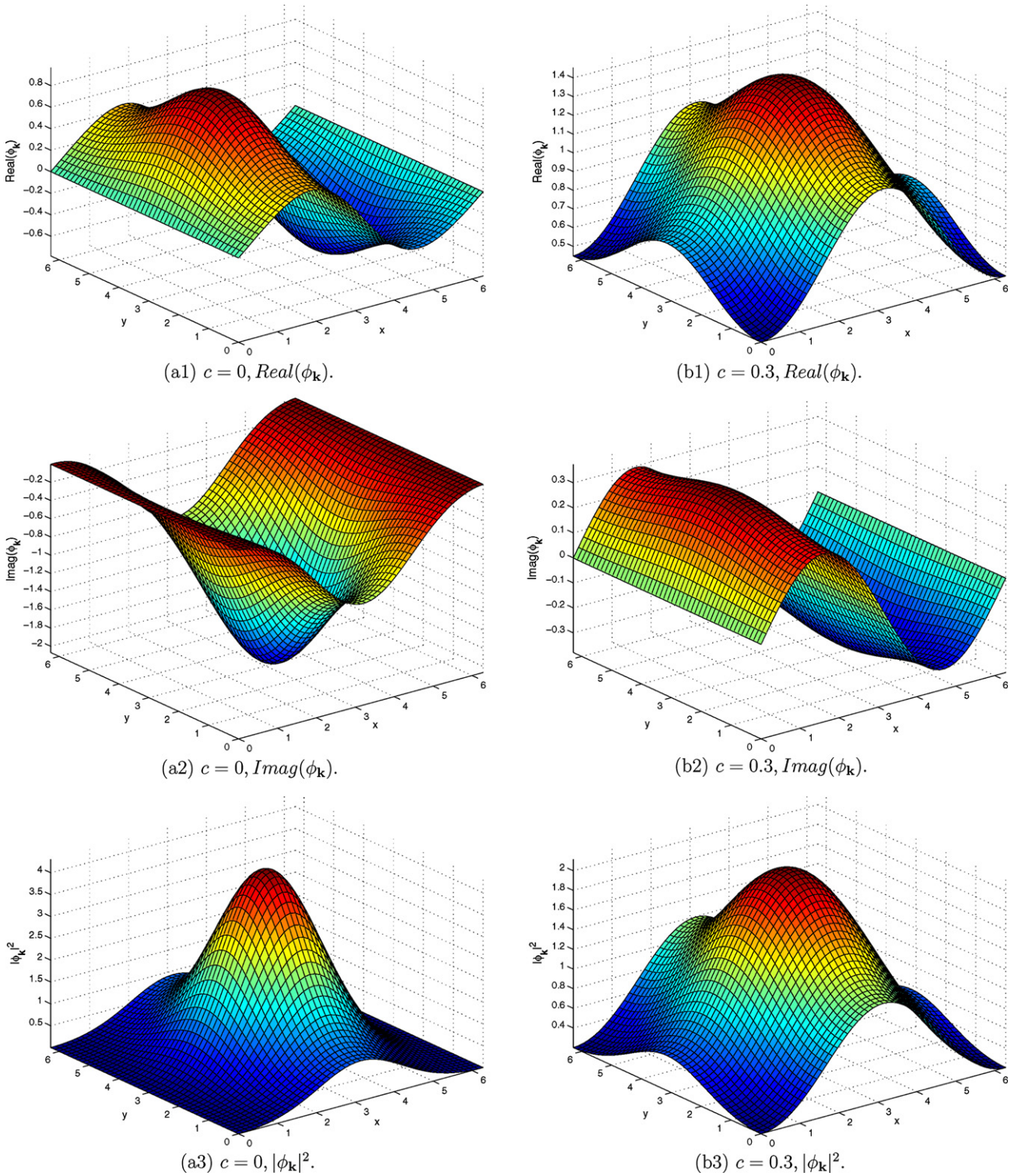

(a1) $c = 0, Real(\phi_{\mathbf{k}})$. (b1) $c = 0.3, Real(\phi_{\mathbf{k}})$.

(a2) $c = 0, Imag(\phi_{\mathbf{k}})$. (b2) $c = 0.3, Imag(\phi_{\mathbf{k}})$.

(a3) $c = 0, |\phi_{\mathbf{k}}|^2$. (b3) $c = 0.3, |\phi_{\mathbf{k}}|^2$.

Fig. 5. The contours of the real part and imaginary part of $\phi_{\mathbf{k}}$ and $|\phi_{\mathbf{k}}|^2$ with linear counterparts at the target points with $\nu = 0.2$, $\mathbf{k} = (k_x, k_y) = (0, 0.5)$, and $c = 0$, $\mu \approx -0.0212969$ (left) and $c = 0.3$, $\mu \approx 0.4145793$ (right).

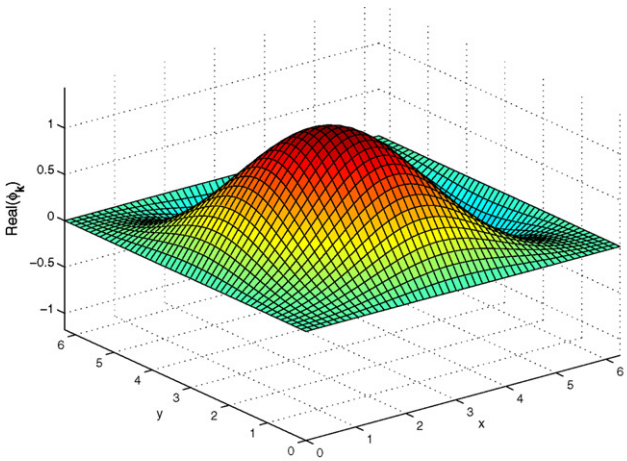

(a1) $c = 0, Real(\phi_{\mathbf{k}})$.

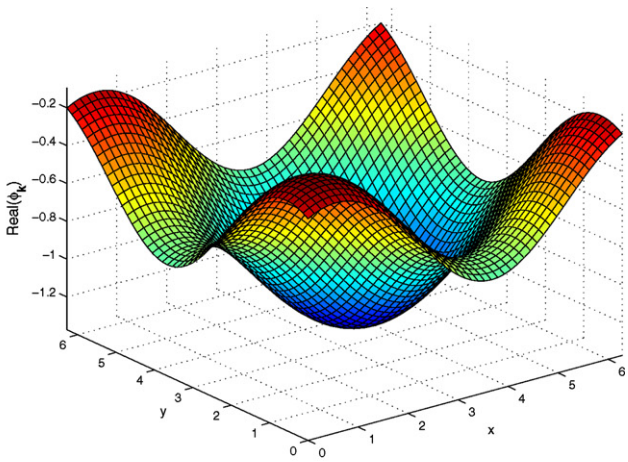

(b1) $c = 0.3, Real(\phi_{\mathbf{k}})$.

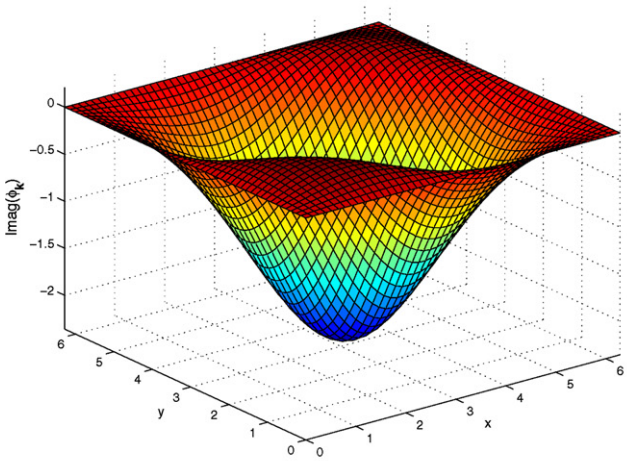

(a2) $c = 0, Imag(\phi_{\mathbf{k}})$.

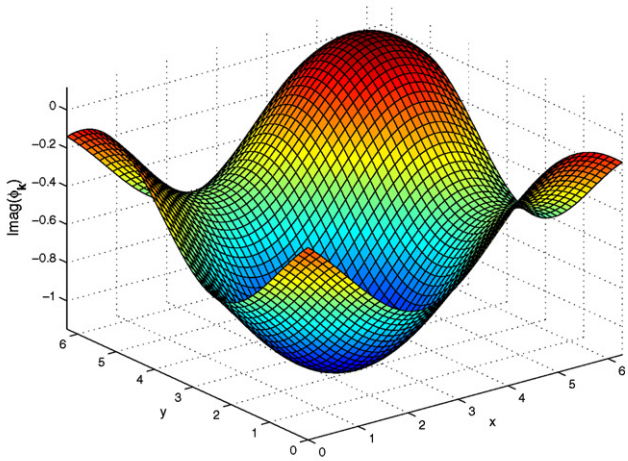

(b2) $c = 0.3, Imag(\phi_{\mathbf{k}})$.

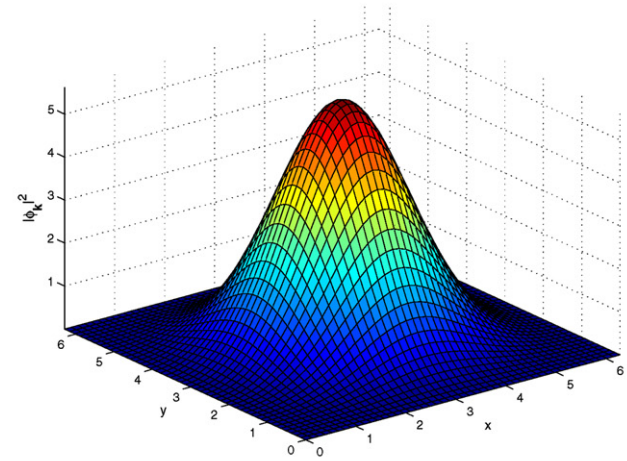

(a3) $c = 0, |\phi_{\mathbf{k}}|^2$.

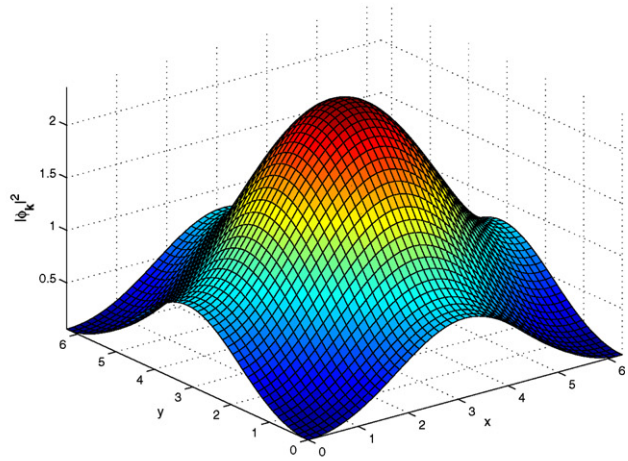

(b3) $c = 0.3, |\phi_{\mathbf{k}}|^2$.

Fig. 6. The contours of the real part and imaginary part of $\phi_{\mathbf{k}}$ and $|\phi_{\mathbf{k}}|^2$ with linear counterparts at the target points with $\nu = 0.2$, $\mathbf{k} = (0.5, 0.5)$, and $c = 0$, $\mu \approx 0.0326021$ (left) and $c = 0.3$, $\mu \approx 0.5412584$ (right).

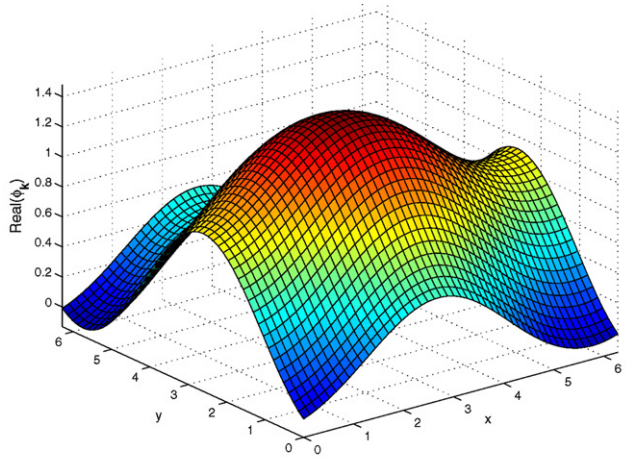

(a1) $\mu \approx 0.57771$, $Real(\phi_{\mathbf{k}})$.

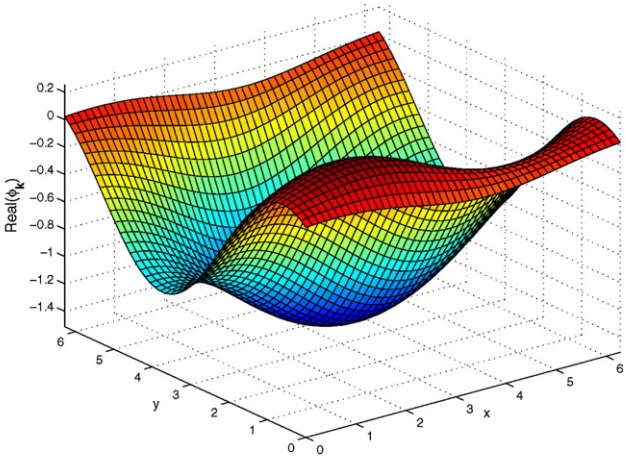

(b1) $\mu \approx 0.58591$, $Real(\phi_{\mathbf{k}})$.

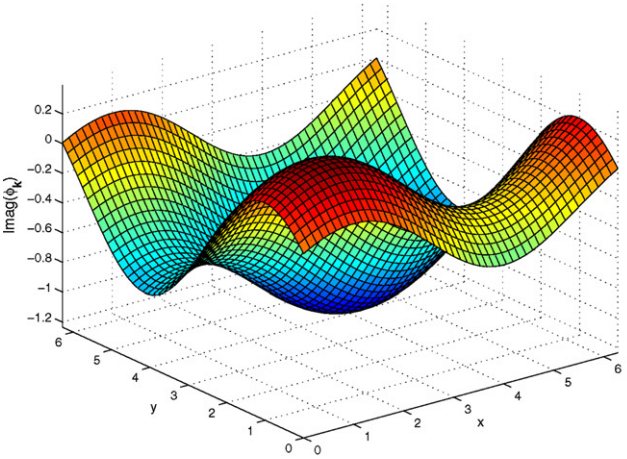

(a2) $\mu \approx 0.57771$, $Imag(\phi_{\mathbf{k}})$.

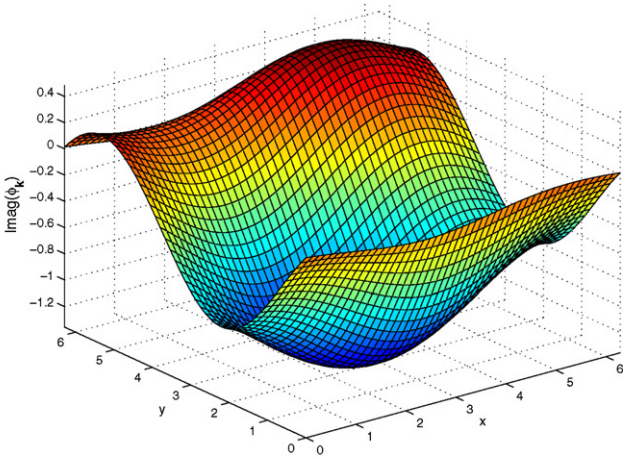

(b2) $\mu \approx 0.58591$, $Imag(\phi_{\mathbf{k}})$.

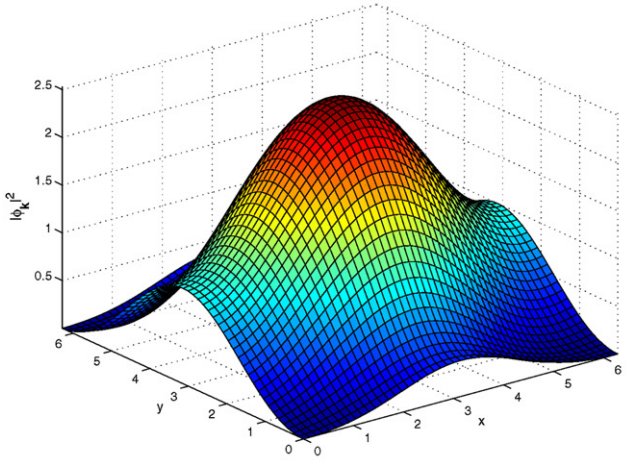

(a3) $\mu \approx 0.57771$, $|\phi_{\mathbf{k}}|^2$.

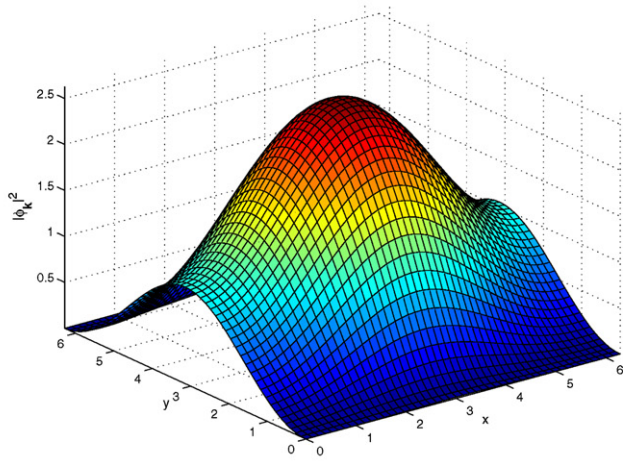

(b3) $\mu \approx 0.58591$, $|\phi_{\mathbf{k}}|^2$.

Fig. 7. The contours of the real part and imaginary part of $\phi_{\mathbf{k}}$ and $|\phi_{\mathbf{k}}|^2$ without linear counterparts at the target points with $\nu = 0.2$, $c = 0.3$, and $\mathbf{k} = (0.54727, 0.5)$, $\mu \approx 0.57771$ (left) and $\mathbf{k} = (0.51306, 0.5)$, $\mu \approx 0.58591$ (right).

[6] V.I. Yukalov, E.P. Yukalova, V.S. Bagnato, Nonlinear coherent modes of trapped Bose–Einstein condensates, Phys. Rev. A 66 (2002) 043602.
[7] B. Wu, Q. Niu, Nonlinear Landau–Zener tunneling, Phys. Rev. A 61 (2000) 023402.
[8] B. Wu, Q. Niu, Landau and dynamical instabilities of the superflow of Bose–Einstein condensates in optical lattices, Phys. Rev. A 64 (2001) 061603.
[9] D. Diakonov, L.M. Jensen, C.J. Pethick, H. Smith, Loop structure of the lowest Bloch band for a Bose–Einstein condensate, Phys. Rev. A 66 (2002) 013604.
[10] E.J. Doedel, et al., AUTO97: Continuation and bifurcation software for ordinary differential equations, available via: ftp://ftp.es.concordia.ca/directory/doedel/auto.
[11] T.R.O. Melvin, A.R. Champneys, P.G. Kevrekidis, J. Cuevas, Radiationless traveling waves in saturable nonlinear Schrödinger lattices, Phys. Rev. Lett. 97 (2006) 124101.
[12] S.-L. Chang, C.-S. Chien, B.-W. Jeng, Computing wave functions of nonlinear Schrödinger equations: a time-independent approach, J. Comput. Phys. 226 (2007) 104–130.
[13] S.-L. Chang, C.-S. Chien, Adaptive continuation algorithms for computing energy levels of rotating Bose–Einstein condensates, Comput. Phys. Commun. 177 (2007) 707–719.
[14] H. Schwetlick, J. Cleve, High order predictors and adaptive steplength control in path following algorithms, SIAM J. Numer. A 24 (1987) 1382–1393.
[15] J.C. Bronski, L.D. Carr, B. Deconinck, J.N. Kutz, Bose–Einstein condensates in standing waves: the cubic nonlinear Schrödinger equation with a periodic potential, Phys. Rev. Lett. 86 (2001) 1402.
[16] J.C. Bronski, L.D. Carr, B. Deconinck, J.N. Kutz, K. Promislow, Bose–Einstein condensates in standing waves: the cubic nonlinear Schrödinger equation with a periodic potential, Phys. Rev. E 63 (2001) 036612.
[17] B. Wu, R.B. Diener, Q. Niu, Bloch waves and Bloch bands of Bose–Einstein condensates in optical lattices, Phys. Rev. A 65 (2002) 025601.
[18] J. Yang, T.I. Lakoba, Accelerated imaginary time evolution methods for the computation of solitary waves, Stud. Appl. Math. 120 (2008) 265–292.
[19] S.-L. Chang, H.-S. Chen, C.-S. Chien, A multigrid continuation algorithm for multiple peak solutions of the Gross–Pitaevskii equation in a periodic potential, preprint, 2010.